On the Energy Efficiency of NOMA for Wireless Backhaul in Multi-Tier Heterogeneous CRAN

Huu Q. Tran[†], Phuc Q. Truong[†], Ca V. Phan[†], Quoc-Tuan Vien[‡]
[†]Ho Chi Minh City University of Technology and Education, Vietnam.
Email: ttdv08@gmail.com; {phuctq; capv}@hcmute.edu.vn
[‡]Middlesex University, United Kingdom. Email: q.vien@mdx.ac.uk

Abstract—This paper addresses the problem of wireless backhaul in a multi-tier heterogeneous cellular network coordinated by a cloud-based central station (CCS), namely heterogeneous cloud radio access network (HCRAN). A non-orthogonal multiple access (NOMA) is adopted in the power domain for improved spectral efficiency and network throughput of the wireless downlink in the HCRAN. We first develop a power allocation for multiple cells of different tiers taking account of the practical power consumption of different cell types and wireless backhaul. By analysing the energy efficiency (EE) of the NOMA for the practical HCRAN downlink, we show that the power available at the cloud, the propagation environment and cell types have significant impacts on the EE performance. In particular, in a large network, the cells located at the cloud edge are shown to suffer from a very poor performance with a considerably degraded EE, which accordingly motivates us to propose an iteration algorithm for determining the maximal number of cells that can be supported in the HCRAN. The results reveal that a double number of cells can be covered in the urban environment compared to those in the shadowed urban environment and more than 1.5 times of the number of microcells can be deployed over the macrocells, while only a half number of cells can be supported when the distance between them increases threefold.

I. INTRODUCTION

Recently, cloud radio access network (CRAN) has emerged as a promising network architecture that enables all base stations (BSs) to be aggregated via the coordination of a cloud-based centralised unit [1], [2]. The CRAN architecture not only enables agility, faster service delivery and cost savings, but also improves the coordination of radio capabilities across a set of remote radio heads (RRHs) with various services, such as interference management and handover control at cell boundaries. Moreover, the CRAN is expected to help reduce the number of cell sites as well as the load at the BSs while still maintaining the network coverage with BS coordination [3]–[5].

In order to improve system throughput and spectral efficiency, non-orthogonal multiple access (NOMA) has been identified as a key enabling multiple access technique for the next generation radio access networks [6]–[9]. With NOMA, multiple users are allowed to be laid over each other in the power domain by allocating different transmission power levels according to user channel conditions while ensuring that all users access the shared wireless medium with the same diversity as in the conventional orthogonal multiple access technique, such as orthogonal frequency division multiple access (OFDMA). Furthermore, in the NOMA, successive interference cancellation (SIC) that allows to receive two or more signals concurrently is employed at each user to recover the interested data packets resulting in not only enhanced reception capacity but also improved cell-edge user throughput [7]–[11].

As an effective and advanced technique, NOMA has been applied and adapted in different network models. In particular, there has been a rich literature using the NOMA technique as a promising candidate to design the air interface for the fifth generation (5G) cellular networks [6], [7]. In our previous work [12], we have first attempted to investigate the NOMA in practical heterogeneous networks[1] integrating with CRAN, namely heterogeneous CRAN (HCRAN). In the HCRAN, BSs of various types, such as macro BSs, micro BSs, remote radio head (RRH) based BSs, pico BSs, femto BSs, etc., are incorporated via a cloud to cooperatively assist the mobile users. However, such high density of BSs may cause severe interference, inefficient resource usage and a considerably degraded throughput at distant cells located at the cloud edge.

In this paper, we first adopt the proposed energy-efficient NOMA for wireless downlink in HCRAN. The proposed NOMA allocates different powers to different BS types depending on their relative distances to the cloud-based central station (CCS) and the channel quality of the wireless links to enhance the spectrum efficiency and achievable throughput. Taking into account different power consumption levels of various BS types and the wireless backhaul in heterogeneous network deployment, we focus on mathematically analysing the achievable throughput and energy efficiency (EE) as well as investigating the impacts of propagation model on the proposed NOMA in the practical HCRAN. Concurrently, extensive simulations are performed to verify the performance of the NOMA. The results show that the EE of the NOMA does not always increase as a function of the number of BSs, but it gradually decreases when the number of BSs exceeds a certain value. Such performance variance depends on many factors, such as propagation environment, power supply at the CCS and the BS types in the HCRAN. In particular, the performance is significantly degraded at the cloud-edge area when deploying a large number of BSs. Therefore, as a second contribution of this paper, we present an iterative method to

---

[1]A heterogeneous cellular network consists of multiple tiers of various cell types, such as macrocells, microcells, picocells, femtocells, etc., for modelling the modern wireless communication systems, e.g. in [13]–[15].

find the maximal number of BSs of various cell types that can be supported in the practical HCRAN under the constraints on the minimum throughput requirement at the cloud-edge area and the limited total power available at the CCS.

II. SYSTEM MODEL

The system model of an HCRAN under investigation consists of K types of BSs, each of which has N_k BSs $\{BS_{k,1}, BS_{k,2}, \ldots, BS_{k,N_k}\}$, $k = 1, 2, \ldots, K$. A CCS is employed as a central unit in the cloud to manage the whole HCRAN. Let d_{k,i_k} denote the distance between the BS_{k,i_k}, $i_k = 1, 2, \ldots, N_k$, and the CCS. All the $\{\mathcal{BS}_{k,i_k}\}$ are assumed to connect to the CCS via wireless backhaul links with perfectly synchronised signalling.

A. Channel Model

Over the wireless medium, the downlink channel from CCS to BS_{k,i_k}, $k = 1, 2, \ldots, K$, $i_k = 1, 2, \ldots, N_k$, is assumed to suffer from flat fading h_{k,i_k} and additive Gaussian noise n_{k,i_k} having $E[|h_{k,i_k}|^2] = 1/d_{k,i_k}^{\nu_{k,i_k}}$ and $E[|n_{k,i_k}|^2] = \sigma_{k,i_k}^2$, where $E[\cdot]$ denotes the statistical expectation function and ν_{k,i_k} denotes the path loss exponent of the propagation model. The signal transmitted from the CCS to BS_{k,i_k} is x_{k,i_k} having $E[|x_{k,i_k}|^2] = 1$.

Let P_{k,i_k} denote the transmission power allocated for the BS_{k,i_k}. The instantaneous signal-to-interference-plus-noise ratio (SINR) at the BS_{k,i_k} (i.e. γ_{k,i_k}) is thus given by

$$\gamma_{k,i_k} = \frac{P_{k,i_k}|h_{k,i_k}|^2}{I_{j \neq i_k} + \sigma_i^2}, \tag{1}$$

where $I_{j \neq i_k}$ denotes the cumulative interference caused by all other BSs except BS_{k,i_k}.

B. Power Consumption Model

It is noticed that the total power consumption for the wireless downlink consists of not only the power consumption of BSs and CCS but also the power consumed by the backhaul [16], [17].

1) Power Consumption of a BS: In a practical cellular network, the power consumption of a BS includes the power for signal processing at baseband (BB) unit, radio frequency (RF) transceiver and power amplifier (PA) as well as considering the power losses caused by DC-DC power supply, mains supply (MS), cooling and inefficiency of the PA[2] [18], [19]. Let $P_k^{(A)}$, $P_k^{(RF)}$ and $P_k^{(BB)}$, $k = 1, 2, \ldots, K$, denote the output radiated power at an antenna element, the RF power and the BB power, respectively, of a k-th type BS. The power consumption of the k-th type BS (i.e. $P_k^{(C)}$) can be determined by

$$P_k^{(C)} = N_k^{(TRX)} \frac{\dfrac{P_k^{(A)}}{\eta_k^{(PA)}\left(1 - \alpha_k^{(feed)}\right)} + P_k^{(RF)} + P_k^{(BB)}}{\left(1 - \alpha_k^{(DC)}\right)\left(1 - \alpha_k^{(MS)}\right)\left(1 - \alpha_k^{(cool)}\right)}, \tag{2}$$

[2]For simplicity, in this paper, the BSs of the same cell type are assumed to have the same power consumption.

where $N_k^{(TRX)}$ is the number of transceiver chains, $\eta_k^{(PA)}$ is the efficiency of the PA, $\alpha_k^{(feed)}$ is the feeder loss, $\alpha_k^{(DC)}$ is the DC-DC power supply loss, $\alpha_k^{(MS)}$ is the MS loss and $\alpha_k^{(cool)}$ is the cooling loss at the k-th type BS.

2) Backhauling Power: The power consumed by wireless backhaul for the downlink from CCS to a BS consists of the power consumed by the downlink interfaces of wireless switches and aggregation switch at the CCS. Let $P_k^{(BH)}$, $k = 1, 2, \ldots, K$, denote the backhauling power of the downlink from CCS to a k-th type BS. With the assumption of identical downlink interfaces and switches at the BSs of the same type, $P_k^{(BH)}$ can be given by [16]

$$P_k^{(BH)} = \frac{\omega_k P_{k,\max}^{(SW)} + (1 - \omega_k)\dfrac{Ag_k^{(SW)}}{Ag_{k,\max}}P_{k,\max}^{(SW)}}{N_k^{(INT)}} + P_k^{(INT)}, \tag{3}$$

where $N_k^{(INT)}$ is the number of interfaces per switch, $P_{k,\max}^{(SW)}$ is the maximum power consumption of switch when all interfaces are used, $P_k^{(INT)}$ is the power consumption of an interface in the aggregation switch, $Ag_k^{(SW)}$ is the amount of traffic passing through the switch and $Ag_{k,\max}$ is the maximum amount of traffic that a switch at the k-th type BS can handle. Here, ω_k is a weighting factor representing the relative influence between the power consumption for the backplane of the switch (i.e. $P_{k,\max}^{(SW)}$) which is independent of the traffic and the power quantity with respect to $Ag_k^{(SW)}$ [17].

Overall, the total power consumption for the downlink in HCRAN is

$$P_{tot} = \sum_{k=1}^{K}\left[N_k\left(P_k^{(C)} + P_k^{(BH)}\right) + \sum_{i_k=1}^{N_k}P_{k,i_k}\right]. \tag{4}$$

III. NOMA AND POWER ALLOCATION IN HCRAN

A. Proposed NOMA for Wireless Downlink in HCRAN

In HCRAN downlink employing NOMA, the signals for $\{BS_{k,i_k}\}$, $k = 1, 2, \ldots, K$, $i_k = 1, 2, \ldots, N_k$, are first superimposed at CCS as follows

$$x = \sum_{k=1}^{K}\sum_{i_k=1}^{N_k}\sqrt{P_{k,i_k}}x_{k,i_k}. \tag{5}$$

Over the fading channel h_{k,i_k}, the signal received at BS_{k,i_k} is

$$y_{k,i_k} = h_{k,i_k}x + n_{k,i_k}, \tag{6}$$

where n_{k,i_k} denotes the complex additive white Gaussian noise at the BS_{k,i_k} having zero mean and variance of σ_{k,i_k}^2.

At BSs, SIC is employed to recover the interested data in a decreasing order of the channel gain. The BS having a higher channel gain is decoded before the one with a lower channel gain. Let G_{k,i_k} denote the normalised channel gain of the link from CCS to BS_{k,i_k} over the noise power. G_{k,i_k} can be given by

$$G_{k,i_k} = \frac{E[|h_{k,i_k}|^2]}{\sigma_{k,i_k}^2} = \frac{1}{d_{k,i_k}^{\nu_{k,i_k}}\sigma_{k,i_k}^2}. \tag{7}$$

It can be observed in (7) that both the distance (i.e. d_{k,i_k}) and the wireless channel propagation model (i.e. ν_{k,i_k}) between CCS and BS_{k,i_k} have significant impacts on G_{k,i_k}, which affects the power allocation as well as when evaluating the achievable throughput and EE of the HCRAN downlink in Section IV.

B. Power Allocation for Wireless Downlink in HCRAN

For simplicity, the noises at BSs of the same cell type are assumed to have the same power (i.e. $\sigma^2_{k,i_k} = \sigma^2_{k,0}$, $\forall k = 1, 2, \ldots, K$, $i_k = 1, 2, \ldots, N_k$). Let us consider the power allocation for the BSs in the k-th type cells[3] and let $P_{k,tot}$ denote the total transmission power at the CCS for these k-th type BSs, i.e.

$$P_{k,tot} = \sum_{i_k=1}^{N_k} P_{k,i_k}. \tag{8}$$

Without loss of generality, assume that $G_{k,1} > G_{k,2} > \cdots > G_{k,N_k}$. The power allocated at the BSs in k-th type cells should therefore satisfy $P_{k,1} < P_{k,2} < \cdots < P_{k,N_k}$. Let us denote λ_{k,i_k}, $i_k = 1, 2, \ldots, N_k - 1$, as the ratio of power allocated for BS_{k,i_k+1} and the power for BS_{k,i_k}, i.e.

$$\lambda_{k,i_k} = \frac{P_{k,i_k+1}}{P_{k,i_k}} = \frac{G_{k,i_k}}{G_{k,i_k+1}} = \frac{d^{\nu_{k,i_k+1}}_{k,i_k+1}}{d^{\nu_{k,i_k}}_{k,i_k}}. \tag{9}$$

Recursively, P_{k,i_k+1} in (9) can be determined by

$$\begin{aligned} P_{k,i_k+1} &= \lambda_{k,i_k} P_{k,i_k} \\ &= \lambda_{k,i_k} \lambda_{k,i_k-1} P_{k,i_k-1} \\ &= \prod_{j=1}^{i_k} \lambda_{k,j} P_{k,1}, \end{aligned} \tag{10}$$

and the power allocated for BS_{k,N_k} can be similarly given by

$$P_{k,N_k} = \prod_{j=1}^{N_k-1} \lambda_{k,j} P_{k,1}. \tag{11}$$

The total transmission power at the CCS for BSs in k-th type cells can be obtained by

$$P_{k,tot} = \sum_{i_k=1}^{N_k} \prod_{j=1}^{i_k-1} \lambda_{k,j} P_{k,1}. \tag{12}$$

The power for $\text{BS}_{k,1}$ can be therefore allocated as

$$P_{k,1} = \frac{P_{k,tot}}{\sum_{i_k=1}^{N_k} \prod_{j=1}^{i_k-1} \lambda_{k,j}}. \tag{13}$$

Substituting (13) into (10), the power for other BS (i.e. BS_{k,i_k}, $i_k = 2, 3, \ldots, N_k$) can be sequentially determined as

$$P_{k,i_k} = \frac{\prod_{j=1}^{i_k-1} \lambda_{k,j}}{\sum_{i_k=1}^{N_k} \prod_{j=1}^{i_k-1} \lambda_{k,j}} P_{k,tot}. \tag{14}$$

---

[3]Note that the power allocation for the whole network can be straightforwardly obtained by individually treating BSs of the same cell type.

IV. PERFORMANCE ANALYSIS AND OPTIMISATION FOR CLOUD EDGE IN HCRAN DOWNLINK

In this section, the throughput and EE of NOMA scheme for wireless downlink in HCRAN are first derived, followed by the introduction of an optimisation problem for supporting cloud-edge area.

A. Throughput and EE of NOMA

Let R and ξ denote the total throughput in bits/s and the EE in bits/J, respectively. The EE is defined as the ratio of the total throughput and the total power consumption in the whole network, i.e.

$$\xi \triangleq \frac{R}{P_{tot}}, \tag{15}$$

where P_{tot} is given by (4).

From (5) and (6), the signal received at BS_{k,i_k}, $k = 1, 2, \ldots, K$, $i_k = 1, 2, \ldots, N_k$, can be rewritten as

$$y_{k,i_k} = \sum_{k=1}^{K} \sum_{i_k=1}^{N_k} h_{k,i_k} \sqrt{P_{k,i_k}} x_{k,i_k} + n_{k,i_k}. \tag{16}$$

Therefore, the achievable throughput, in bits/s, at BS_{k,i_k} with NOMA can be computed by

$$R_{k,i_k} = W \log_2 \left(1 + \frac{P_{k,i_k} |h_{k,i_k}|^2}{\sum_{j=1}^{i_k-1} P_{k,j} |h_{k,j}|^2 + \sigma^2_k} \right), \tag{17}$$

where W denotes the transmission bandwidth. The total achievable throughput is thus given by

$$R = \sum_{k=1}^{K} \sum_{i_k=1}^{N_k} W \log_2 \left(1 + \frac{P_{k,i_k} |h_{k,i_k}|^2}{\sum_{j=1}^{i_k-1} P_{k,j} |h_{k,j}|^2 + \sigma^2_k} \right). \tag{18}$$

The EE of NOMA for the downlink in the HCRAN can be determined by substituting (18) and (4) into (15) as

$$\xi = \frac{\displaystyle\sum_{k=1}^{K} \sum_{i_k=1}^{N_k} W \log_2 \left(1 + \frac{P_{k,i_k} |h_{k,i_k}|^2}{\sum_{j=1}^{i_k-1} P_{k,j} |h_{k,j}|^2 + \sigma^2_k} \right)}{\displaystyle\sum_{k=1}^{K} \left[N_k \left(P_k^{(C)} + P_k^{(BH)} \right) + \sum_{i_k=1}^{N_k} P_{k,i_k} \right]}. \tag{19}$$

B. Optimisation Problem for Supporting Cloud-Edge Area

As shown in (19), the performance of the NOMA scheme depends on the number of BSs/cells of different types. In fact, a very large number of cells cause a low EE and considerably degraded throughput at the cloud-edge area.

For simplicity, let us assume that the number of cell types (i.e. K) in HCRAN is known and invariant. The objective in the optimisation problem is to find the maximal number of the BSs of each cell type that can be supported subject to the constraints on the minimum throughput requirement at cloud edge and the limited power available at the CCS. We can formulate the optimisation problem for BSs of k-th cell type, $k = 1, 2, \ldots, K$, as follows:

$$\max N_k \tag{20}$$

s.t.

$$\sum_{i_k=1}^{N_k} P_{k,i_k} \leqslant P_{k,\max}, \tag{21}$$

$$W \log_2 \left(1 + \frac{P_{k,N_k}|h_{k,N_k}|^2}{\sum_{j=1}^{N_k-1} P_{k,j}|h_{k,j}|^2 + \sigma_k^2} \right) \geq R_{k,thre}, \tag{22}$$

where $P_{k,\max}$ is the maximum power allocated for the BSs of the k-th cell type, $R_{k,thre}$ is the cloud-edge throughput threshold and the LHS of the constraint (22) corresponds to the throughput at the cloud edge (i.e. R_{k,N_k} given by (17) when $i_k = N_k$).

For convenience, let $N_{k,\max}$ denote the maximal number of the k-th type BSs. The finding of $N_{k,\max}$ can be realised with an iterative search algorithm as summarised in Algorithm 1. The corresponding EE can be then determined by (19) with $N_k = N_{k,\max}$.

Algorithm 1 Maximal Number of BSs in HCRAN

1: **for** $k = 1$ **to** K **do**
2:    $N_{k,\max} \leftarrow 0$
3:    $j \leftarrow 0$
4:    **repeat**
5:       $j \leftarrow j + 1$
6:       Find $\{P_{k,i_k}\}$, $i_k = 1, 2, \ldots, j$, using (14).
7:       Find $R_{k,j}$ using (17).
8:    **until** $R_{k,j} < R_{k,thre}$
9:    $N_{k,\max} \leftarrow j - 1$
10: **end for**

V. NUMERICAL RESULTS

In this section, we analyse the performance of the proposed NOMA for wireless downlink in a multi-tier HCRAN under various operating conditions as well as indicating the maximal number of BSs/cells of different types that can be supported. In particular, we consider three BS types (i.e. $K = 3$), including macro, RRH and micro BSs, and two propagation environment having path loss exponents of $\nu = 2.4$ and $\nu = 3$ representing urban and shadowed urban cellular radio environment, respectively. The transmission bandwidth is set as $W = 10$ MHz.

For power consumption modelling, using (2) with simulation parameters for the LTE BSs as in [18], the power consumption of macro, RRH and micro BSs can be determined as $P_1^{(C)} = 1350$ W, $P_2^{(C)} = 754.8$ W and $P_3^{(C)} = 144.6$ W, respectively. Regarding the backhaul, we assume that there are 24 interfaces per switch, the maximum power consumption of a switch is 300 W, the power consumption of a downlink interface in the aggregation switch is 1 W, weighting factor is 0.5, the amount of traffic passing through the switch is 1 Gbits/s and the maximum amount of traffic that a switch can handle is 24 Gbits/s.

For convenience, Table I summarises relevant simulation parameters and their default values if otherwise stated.

TABLE I: Parameter values used in the simulations results.

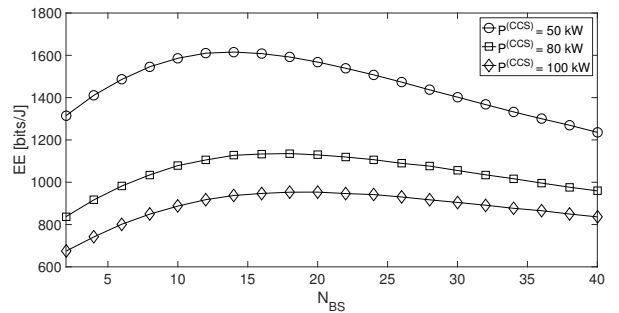| Parameters	Value (default)
Number of cell types	3
Macro BS power consumption ($P_1^{(C)}$)	1350 W
RRH power consumption ($P_2^{(C)}$)	754.8 W
Micro BS power consumption ($P_3^{(C)}$)	144.6 W
Maximum switch power consumption	300 W
Downlink interface power consumption	1 W
Interfaces per switch	24
Maximum traffic of a switch	24 Gbps
Weighting factor	0.5
Transmission bandwidth	10 MHz

Fig. 1: EE of NOMA versus the number of BSs w.r.t. various power allocated at CCS.

A. Performance of NOMA in HCRAN Downlink

1) Impact of power allocation at CCS: We first analyse the impact of power allocation at CCS on the performance of the proposed NOMA for wireless downlink in HCRAN. Fig. 1 plots the EE versus the number of BSs with respect to different values of power supply available at the CCS (i.e. $P^{(CCS)}$). Specifically, three scenarios of $P^{(CCS)} = \{100, 80, 50\}$ kW are considered for urban cellular network model with $\nu = 2.4$. We assume that the distances between the BSs and CCS are in the range of 100 m to 8 km with an interval of 200 m corresponding to the channel gain from 20 dB to 0 dB with a decrement factor of $1/2$. It can be observed in Fig. 1 that, as long as the CCS is able to support the BSs, only a low power is required at the CCS, and thus results in the highest EE performance. Also, the maximal performance is shown to be achieved at a specific number of BSs according to the power available at the CCS, while the performance is considerably degraded when the number of BSs is either too small or too large.

2) Impact of BS types: Figure 2 illustrates the impact of BS types on the EE of NOMA in HCRAN downlink. Specifically, three BS types including macro BSs, RRHs and micro BSs, are considered. The deployment of micro BSs is shown to achieve the best EE performance, especially in a large network, while the same EE can be achieved with any BS types in a small network. In fact, this is due to the difference in power
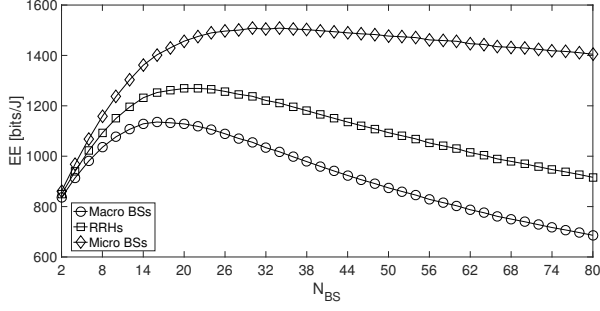
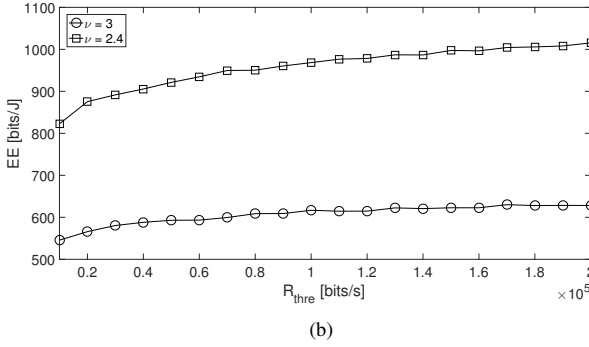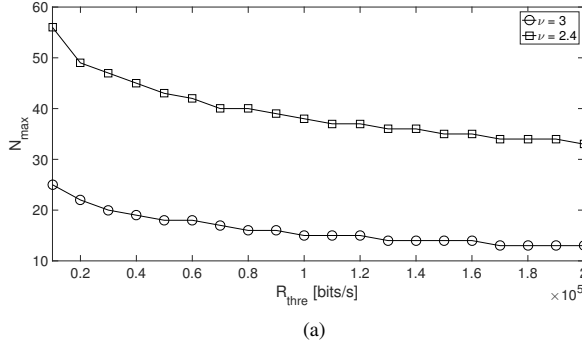Fig. 2: EE of NOMA versus the number of BSs w.r.t. various BS types.

(a)

(b)

Fig. 3: (a) Maximal number of BSs and (b) EE versus cloud-edge throughput threshold w.r.t. various propagation path loss exponents.

(a)

(b)

Fig. 4: (a) Maximal number of BSs and (b) EE versus cloud-edge throughput threshold w.r.t. various distances between cells.

consumption at the BSs of different types. This accordingly reflects the remarkable impact of BS types and their quantity on the performance of the HCRAN.

B. Maximal Number of BSs in HCRAN

This subsection exemplifies the maximal number of BSs that can be supported and the corresponding EE of NOMA in HCRAN downlink taking into account various scenarios of propagation environment, distance between cells and cell types. Note that the maximal number of BSs is hereafter determined by employing Algorithm 1.

1) Impact of propagation environment: Figures 3(a) and 3(b) sequentially illustrate the maximal number of BSs and the
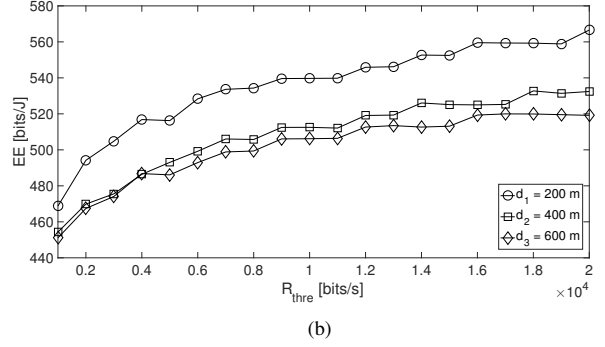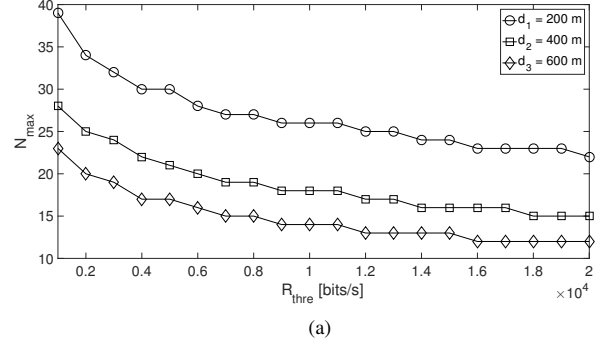
corresponding EE as a function of the cloud-edge throughput threshold considering both urban and shadowed urban environment. It can be observed that the maximal number of BSs operating in both environment decreases as the target cloud-edge throughput increases. In addition, as shown in Fig. 3, the urban model can support a double number of BSs with a higher EE compared to shadowed urban model.

2) Impact of distance between cells: In Figs. 4(a) and 4(b), the maximal number of BSs and the corresponding EE are respectively plotted against the cloud-edge throughput threshold with respect to three scenarios of the distances between cells including $\{200, 400, 600\}$ m. It can be seen in Fig. 4 that, to cover the cloud-edge area, an increased distance between the cells requires a reduced number of BSs in the HCRAN. Specifically, only a half number of the BSs can be supported when the distance between them increases three times.

3) Impact of cell types: Figure 5 illustrates the impact of cell types on the maximal number of BSs and the corresponding EE of NOMA in HCRAN downlink. Similarly, macro BSs, RRHs and micro BSs are considered. As can be seen in Figs. 5(a) and 5(b), the more power the BSs consume. the smaller number of them can be supported providing a higher EE. For instance, more than 1.5 times of the number of micro BSs can be employed compared to the macro BSs.
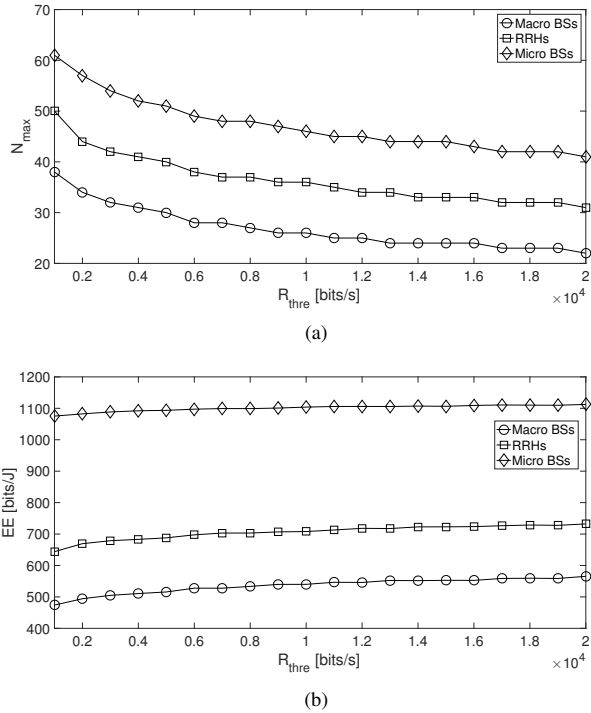
Fig. 5: (a) Maximal number of BSs and (b) EE versus cloud-edge throughput threshold w.r.t. various BS types.

VI. CONCLUSIONS

We have proposed a NOMA scheme for HCRAN downlink taking into account the practical channel modelling, power consumption of various BS types and backhauling power consumption. A heuristic iterative search algorithm has been developed to find the maximal number of BSs of every cell type that can be supported subject to the limited total power and cloud-edge throughput constraint. It has been shown that, given a minimum cloud-edge throughput requirement, the urban environment can support a double number of BSs over the shadowed urban environment and more than 1.5 times of the number of microcells can be accommodated compared to that of the macrocells, while the number of cells should be reduced by half when the distance between them increases threefold.

REFERENCES

[1] J. Wu, Z. Zhang, Y. Hong, and Y. Wen, "Cloud radio access network (C-RAN): a primer," *IEEE Netw.*, vol. 29, no. 1, pp. 35–41, Jan. 2015.
[2] White Paper, "C-RAN: The road towards green RAN," China Mobile Labs, Ver. 3.0, Dec. 2013.
[3] Z. Ding and H. Poor, "The use of spatially random base stations in cloud radio access networks," *IEEE Signal Process. Lett.*, vol. 20, no. 11, pp. 1138–1141, Nov. 2013.
[4] M. Peng, Y. Li, J. Jiang, J. Li, and C. Wang, "Heterogeneous cloud radio access networks: a new perspective for enhancing spectral and energy efficiencies," *IEEE Wireless Commun. Mag.*, vol. 21, no. 6, pp. 126–135, Dec. 2014.
[5] Q.-T. Vien, N. Ogbonna, H. X. Nguyen, R. Trestian, and P. Shah, "Non-orthogonal multiple access for wireless downlink in cloud radio access networks," in *Proc. IEEE EW 2015*, Budapest, Hungary, May 2015, pp. 434–439.
[6] Z. Ma, Z. Ding, P. Fan, and S. Tang, "A general framework for MIMO uplink and downlink transmissions in 5G Multiple Access, year=2016, pages=1-4, month=May, address=Nanjing, China." in *Proc. IEEE VTC Spring 2016*.
[7] L. Dai, B. Wang, Y. Yuan, S. Han, C. l. I, and Z. Wang, "Non-orthogonal multiple access for 5G: solutions, challenges, opportunities, and future research trends," *IEEE Commun. Mag.*, vol. 53, no. 9, pp. 74–81, Sep. 2015.
[8] A. Benjebbour, Y. Saito, Y. Kishiyama, A. Li, A. Harada, and T. Naka-mura, "Concept and practical considerations of non-orthogonal multiple access (NOMA) for future radio access," in *Proc. ISPACS 2013*, Oki-nawa, Japan, Nov. 2013, pp. 770–774.
[9] Y. Saito, Y. Kishiyama, A. Benjebbour, T. Nakamura, A. Li, and K. Higuchi, "Non-orthogonal multiple access (NOMA) for cellular future radio access," in *Proc. IEEE VTC 2013-Spring*, Dresden, Germany, Jun. 2013, pp. 1–5.
[10] H. Osada, M. Inamori, and Y. Sanada, "Non-orthogonal access scheme over multiple channels with iterative interference cancellation and fractional sampling in MIMO-OFDM receiver," in *Proc. IEEE VTC 2013-Fall*, Las Vegas, USA, Sep. 2013, pp. 1–5.
[11] N. Otao, Y. Kishiyama, and K. Higuchi, "Performance of non-orthogonal access with SIC in cellular downlink using proportional fair-based resource allocation," in *Proc. ISWCS 2012*, Paris, France, Aug. 2012, pp. 476–480.
[12] Q.-T. Vien, T. A. Le, B. Barn, and C. V. Phan, "Optimising energy efficiency of non-orthogonal multiple access for wireless downlink in heterogeneous cloud radio access network," *to appear in IET Commun. - Special Issue: "Green Computing and Telecommunications Systems"*, 2016.
[13] T. E. Bogale and L. B. Le, "Massive MIMO and mmWave for 5G wireless hetnet: Potential benefits and challenges," *IEEE Veh. Technol. Mag.*, vol. 11, no. 1, pp. 64–75, Mar. 2016.
[14] Q.-T. Vien, T. Akinbote, H. X. Nguyen, R. Trestian, and O. Gemikonakli, "On the coverage and power allocation for downlink in heterogeneous wireless cellular networks," in *Proc. IEEE ICC 2015*, London, UK, Jun. 2015, pp. 4641–4646.
[15] Q.-T. Vien, T. A. Le, H. X. Nguyen, and M. Karamanoglu, "An energy-efficient resource allocation for optimal downlink coverage in heterogeneous wireless cellular networks," in *Proc. IEEE ISWCS 2015*, Brussels, Belgium, Aug. 2015, pp. 156–160.
[16] S. Tombaz, P. Monti, K. Wang, A. Vastberg, M. Forzati, and J. Zander, "Impact of backhauling power consumption on the deployment of heterogeneous mobile networks," in *Proc. IEEE GLOBECOM 2011*, Houston, TX, USA, Dec. 2011, pp. 1–5.
[17] O. Onireti, F. Heliot, and M. Imran, "On the energy efficiency-spectral efficiency trade-off of distributed MIMO systems," *IEEE Trans. Commun.*, vol. 61, no. 9, pp. 3741–3753, Sep. 2013.
[18] G. Auer, V. Giannini, C. Desset, I. Godor, P. Skillermark, M. Olsson, M. Imran, D. Sabella, M. Gonzalez, O. Blume, and A. Fehske, "How much energy is needed to run a wireless network?" *IEEE Wireless Commun. Mag.*, vol. 18, no. 5, pp. 40–49, Oct. 2011.
[19] B. H. Jung, H. Leem, and D. K. Sung, "Modeling of power consumption for macro-, micro-, and RRH-based base station architectures," in *Proc. IEEE VTC 2014-Spring*, Seoul, Korea, May 2014, pp. 1–5.